EARTHQUAKE ENGINEERING AND STRUCTURAL DYNAMICS
*Earthquake Engng. Struct. Dyn.* **28**, 671–686 (1999)

# A NON-LINEAR NUMERICAL MODEL OF THE TUNED LIQUID DAMPER

JIN-KYU YU[1,†,‡], TOSHIHIRO WAKAHARA[2,‡] AND DOROTHY A. REED[3,*,§]

[1]*Skilling, Ward, Magnusson, Barkshire, Inc., Seattle, WA 98195, U.S.A.*
[2]*Institute of Technology, Shimizu Corporation, Tokyo, Japan,*
[3]*Department of Civil Engineering, University of Washington, Seattle, WA 98195, U.S.A.*

## SUMMARY

The Tuned Liquid Damper (TLD) is modelled numerically as an equivalent tuned mass damper with non-linear stiffness and damping. These parameters are derived from extensive experimental results described in References 1 and 2. This Non-linear Stiffness and Damping (NSD) model captures the behaviour of the TLD system adequately under a variety of loading conditions. In particular, the NSD model incorporates the stiffness hardening property of the TLD under large amplitude excitation. Copyright © 1999 John Wiley & Sons, Ltd.

KEY WORDS: tuned liquid damper; non-linear stiffness and damping model; large amplitude excitation

## INTRODUCTION

The tuned liquid damper has been used in a wide variety of applications as a passive or semi-active structural control device (e.g. References 3–7). Despite this acceptance, the TLD has not been subject to the same level of analytical scrutiny as the solid mass damper, nor has its behaviour under large amplitude excitation more representative of earthquake motion been investigated until recently.[1,2] Previously, analogies with solid mass systems have been made to characterize the behaviour of the liquid systems (e.g. References 4, 7 and 8). In these analogies, the non-linearities of the liquid dampers were based upon limited small excitation amplitude data, and extrapolation to more realistic conditions was made cautiously. Although the use of numerical simulation of the sloshing motion under large amplitude excitation using the shallow water wave equations has been successfully accomplished,[1,2] this model does not provide an effective design tool in its present form.

In this paper, the tuned liquid damper is modelled as an equivalent solid mass damper with non-linear stiffness and damping. This model is a significant expansion of those typically used for

* Correspondence to: Dorothy A. Reed, Department of Civil and Environmental Engineering, Box 352700, University of Washington, Seattle, WA 98195-2700, U.S.A.
† Formerly Graduate Research Assistant, University of Washington, Seattle, WA 98195, U.S.A.
‡ Structural Engineer
§ Professor

Contract/grant sponsor: U.S. National Science Foundation

CCC 0098–8847/99/060671–16$17·50

*Received 30 April 1998*
*Revised 23 December 1998*

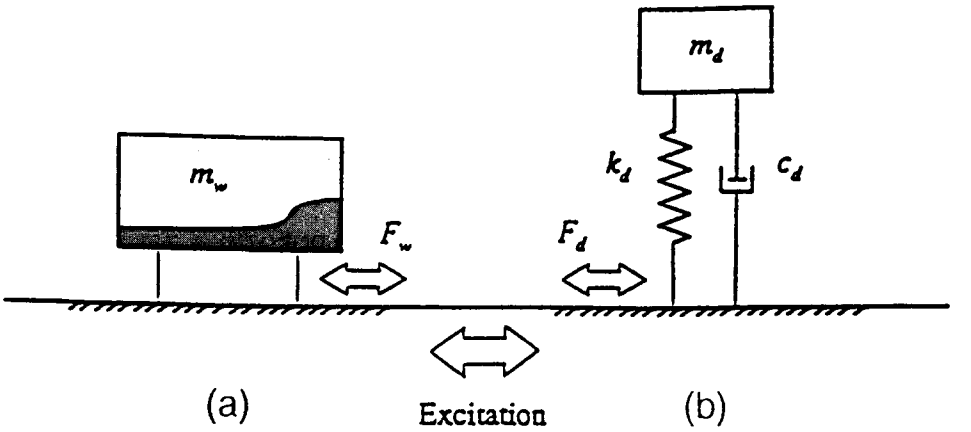


Figure 1. A schematic of the TLD characterized as the NSD model. (a) TLD; (b) NSD model

mass dampers and the non-linear characteristics are calibrated based upon shaking table tests described in detail in Reference 9. It will be shown that this mechanical model adequately characterizes the performance of the TLD for a wide range of amplitudes of excitation. This simple approach has merit as a design tool and may ultimately provide insight into the physical phenomenon of energy dissipation through liquid sloshing.

Figure 1 provides an illustration of the Non-linear-Stiffness-Damping (NSD) model as a Single-Degree-of-Freedom (SDOF) system with stiffness and damping parameters, $k_d$ and $c_d$, respectively. These are determined such that the energy dissipation provided by the NSD is equivalent to that of the TLD. The design challenge is to transform the appropriate parameter set derived for the equivalent solid mass damper into the liquid damper system. The complexities associated with this exercise will be revisited in the section on results. First, the method for estimating the NSD parameters from the empirical data of previous investigations is outlined in the next section.

## PROCEDURE FOR PARAMETER IDENTIFICATION

As shown in Figure 1, the mechanical model of the TLD used for numerical simulation is based upon the development of a control force created by the sloshing motion of the liquid in the tank. In treating the TLD as an equivalent linear system, this force will be characterized by its amplitude and phase. Therefore, the matching scheme must incorporate the combined effect of these two properties. The single parameter of energy dissipation per cycle $E_d$ can be used to match this combination as by definition it is the area inside the loop of the control force vs. the tank base displacement contour. This quantity incorporates the combined effects of amplitude and phase of the control force on the structural motion over the period of one cycle. Data obtained by shaking table experiments described in detail in References 1, 2 and 9 were available for use in quantifying energy dissipation by the control system. Table I contains information concerning the geometric

 

Table I. Data for the rectangular tanks discussed in detail in References 1, 2 and 9

| Case ID | Tank size | | Water depth | Water frequency | Excitation amplitude | |
|---|---|---|---|---|---|---|
| | length $L$ (mm) | width $B$ (mm) | $h_0$ (mm) | $f_w$ (Hz) | $A$ (mm) | $A/L$ |
| L335h9·6 | 335 | 203 | 9·6 | 0·457 | 10 | 0·030 |
| L33h15 | 335 | 203 | 15 | 0·571 | 2·5, 5, 10, 20, 30 | 0·007–0·119 |
| L590h15 | 590 | 335 | 15 | 0·325 | 2·5, 5, 10, 20, 30, 40 | 0·004–0·068 |
| L590h22·5 | 590 | 335 | 22·5 | 0·397 | 2·5, 5, 10, 20, 30, 40 | 0·004–0·068 |
| L590h30 | 590 | 335 | 30 | 0·458 | 2·5, 5, 10, 20, 30, 40 | 0·004–0·068 |
| L590h45 | 590 | 335 | 45 | 0·558 | 20 | 0·034 |
| L900h30 | 900 | 335 | 30 | 0·301 | 2·5, 5, 10, 20, 30, 40 | 0·003–0·044 |
| L900h40 | 900 | 335 | 40 | 0·347 | 2·5, 5, 10, 20, 30, 40 | 0·003–0·044 |
| L900h55 | 900 | 335 | 55 | 0·406 | 10, 20 | 0·011–0·022 |
| L900h71 | 900 | 335 | 71 | 0·459 | 2·5, 5, 10 | 0·003–0·011 |

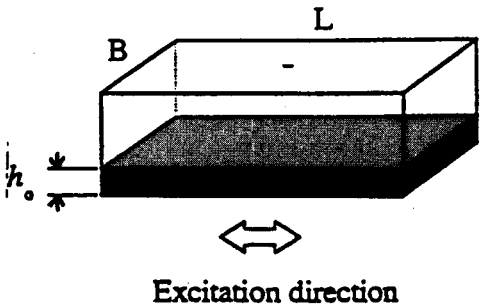


Figure 2. Schematic of the typical rectangular TLD

properties of these tanks and the corresponding range of excitation amplitudes of the shaking table experiments for each tank. A schematic of the typical tank is shown in Figure 2.

Figure 3 presents typical sweep frequency plots of the non-dimensional energy dissipation per cycle for the TLD with length $L = 590$ mm, water depth $h_0 = 30$ mm and excitation amplitude $A = 20$ mm and for its corresponding NSD model. The non-dimensional energy dissipation curve for the TLD, $E'_w$ (solid line) is determined from measurements of the shaking table experiments. It is defined as

$$E'_w = \frac{E_w}{(1/2)m_w(\omega A)^2} \tag{1}$$

where $m_w$ is the mass of the liquid, $\omega$ is the excitation angular frequency of the shaking table, $A$ is the amplitude of the sinusoidal excitation and the denominator of (1) is the maximum kinetic

 

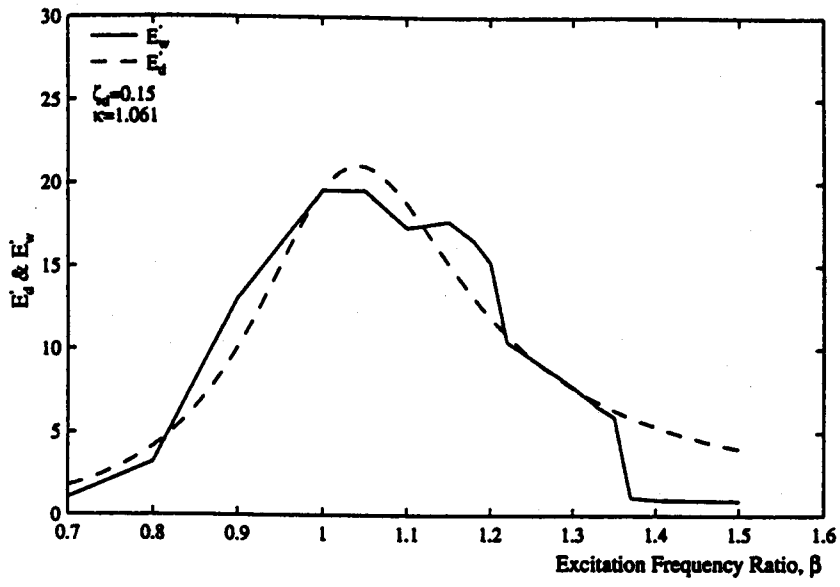


Figure 3. Plots of the non-dimensional energy dissipation curves from the shaking table tests and the NSD model

energy of the water mass treated as a solid mass. The numerator is the energy dissipation per cycle as defined as

$$E_w = \int_{T_s} F_w \, dx \tag{2}$$

with, $dx$ referring to integration over the shaking table displacement per cycle, $F_w$ is the force generated by the liquid sloshing motion in the tank.

The expression for the non-dimensional energy dissipation for the corresponding NSD model $E'_d$ (dashed line) is determined from the analysis of its behaviour when subjected to harmonic base excitation. Specifically, under a harmonic base excitation with frequency ratio $\beta$, the amplitude $|F'_d|$ and the phase $\phi$ of the control force of the NSD are expressed, respectively, in non-dimensional form as follows:

$$|F'_d| = \frac{\sqrt{(1+(4\zeta_d^2-1)\beta^2)^2 + 4\zeta_d^2\beta^6}}{1+(4\zeta_d^2-2)\beta^2+\beta^4} \tag{3a}$$

$$\phi = \tan^{-1}\left[\frac{2\zeta_d\beta^3}{-1+(1-4\zeta_d^2)\beta^2}\right] \tag{3b}$$

where $\beta$ is the excitation frequency ratio as defined by $\beta = f_e/f_d$, $f_e$ is the excitation frequency, $f_d$ is the natural frequency of the NSD defined by $f_d = (1/2\pi)\sqrt{k_d/m_d}$, $\zeta_d$ is the damping ratio of the NSD model defined as $\zeta_d = c_d/c_{cr}$, $c_{cr}$ is the critical damping coefficient defined by $c_{cr} = 2m_d\omega_d$, $\omega_d$ is the linear fundamental natural angular frequency defined as $\omega_d = 2\pi f_d$ and $m_d$, $k_d$ and $c_d$ are the mass, and stiffness and damping coefficients of the NSD model, respectively.

The non-dimensional energy dissipation for the NSD model at each excitation frequency is obtained by the formula

$$E'_d = 2\pi |F'_d| \sin \phi \tag{4}$$

$E'_d$ is fit to $E'_w$ by the least-squares method over the frequency range of high-frequency dissipation. In this scheme,

$$m_d = m_w$$

Beginning with initial estimates of $\zeta_d$ and $f_d$, the scheme determines values of the stiffness and damping coefficients for the experimental cases outlined in Table I. In analysing the results, it is useful to evaluate the stiffness changes through two ratios.

The first is the frequency shift ratio $\xi$, defined as

$$\xi = \frac{f_d}{f_w} \tag{5}$$

where $f_w$ is the linear fundamental natural frequency for a liquid of water depth $h_0$ in a rectangular tank of length $L$ defined by Lamb[10] as

$$f_w = \frac{1}{2\pi} \sqrt{\frac{\pi g}{L} \tanh\left(\frac{\pi h_0}{L}\right)} \tag{6}$$

The parameter $g$ is the gravitational constant. Second, the stiffness hardening ratio $\kappa$ is defined as

$$\kappa = \frac{k_d}{k_w} \tag{7}$$

where $k_w = m_w(2\pi f_w)^2$.

Because $m_d = m_w$,

$$\kappa = \xi^2 \tag{8}$$

## RESULTS

The matching scheme discussed in the previous section was applied to the experimental cases for rectangular TLDs described in Table I to determine damping and stiffness coefficients of the NSD model for a wide range of amplitudes of excitation. Extensive investigation into the characterization of the damping and stiffness as functions of wave height, water depth, amplitude of excitation and tank size was also undertaken. It was found that the non-dimensional amplitude defined as

$$\Lambda = \frac{A}{L} \tag{9}$$

where $A$ is the amplitude of excitation and $L$ is the length of the tank in the corresponding direction of motion provided the most adequate characterization. The results of the NSD matching scheme for the damping and stiffness data are shown in Figures 4 and 5, respectively, as functions of this non-dimensional amplitude. Figure 4 shows the best-fitted curve for the damping parameter $\zeta_d$ as

$$\zeta_d = 0{\cdot}5\Lambda^{0{\cdot}35} \tag{10}$$

 

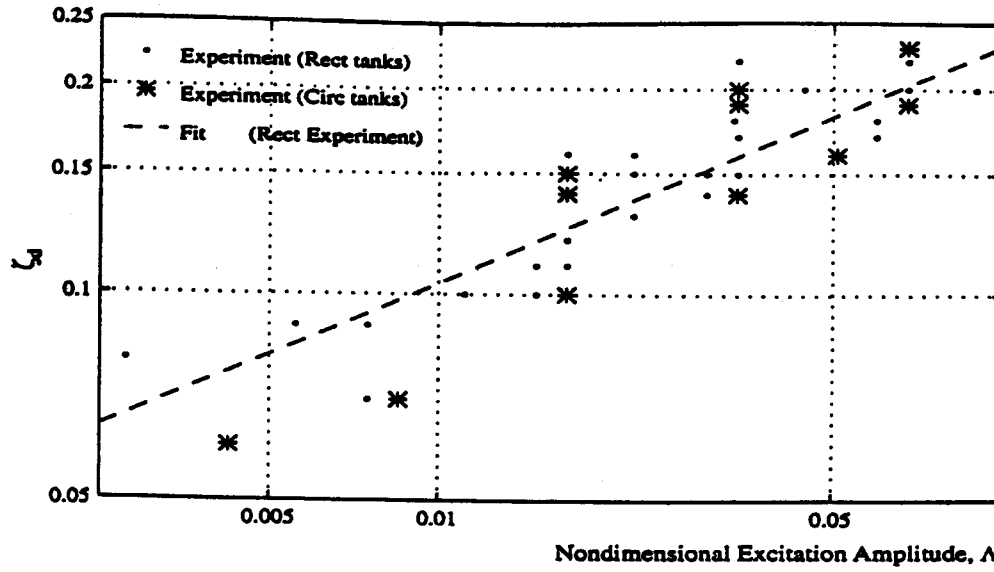


Figure 4. The damping ratio of the NSD model

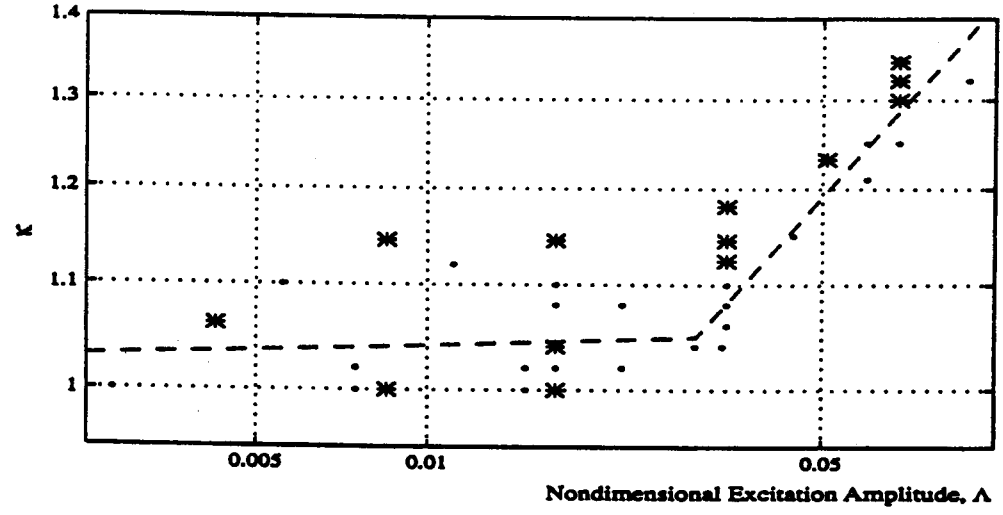


Figure 5. The stiffness hardening ratio

The stiffness hardening ratio $\kappa$ was plotted as a function of the non-dimensional amplitude in Figure 5. This plot shows two distinct regions divided at $\Lambda = 0{\cdot}03$, where the slope changes dramatically. Modified wave behaviour at $\Lambda = 0{\cdot}03$ is consistent with the well-known 'jump' frequency phenomenon for TLDs (e.g. References 11, 12, 1 and 2). The two regions are defined

 

here as *weak* and *strong* wave breaking, respectively. The regression results for these regions using the least-squares method are

$$\kappa = 1{\cdot}075\Lambda^{0{\cdot}007} \quad \text{for } \Lambda \leqslant 0{\cdot}03 \quad \text{weak wave breaking} \tag{11a}$$

and

$$\kappa = 2{\cdot}52\Lambda^{0{\cdot}25} \quad \text{for } \Lambda > 0{\cdot}03 \quad \text{strong wave breaking} \tag{11b}$$

The stiffness hardening ratio increases very slowly with the amplitude of excitation in the weak wave breaking region. In contrast, it changes rapidly in the strong wave breaking region. Noticing the relationship between $\xi$ and $\kappa$ as

$$\xi = \sqrt{\kappa} \tag{12}$$

the frequency shift ratio may be expressed as

$$\xi = 1{\cdot}038\Lambda^{0{\cdot}0034} \quad \text{for } \Lambda \leqslant 0{\cdot}03 \quad \text{weak wave breaking} \tag{13a}$$

and

$$\xi = 1{\cdot}59\Lambda^{0{\cdot}125} \quad \text{for } \Lambda > 0{\cdot}03 \quad \text{strong wave breaking} \tag{13b}$$

Clearly, the stiffness-hardening property of the TLD system is captured in this analysis.

*Comparison with Sun et al.*[8]

In the experimental investigation from which the results shown in Figures 4 and 5 were obtained, the videotaped motion clearly shows a difference in the liquid behaviour in the weak and strong wave breaking regions.[13] Specifically, the taped results show that the effective mass involved in strong wave breaking is higher than that for weak wave breaking. Sun *et al.*[8] observed similar liquid behaviour for specimens under small amplitude excitation, whereby 80 per cent of the total mass was effectively involved initially in wave breaking but increased with amplitude of excitation $A$. The exact amount of mass participation was also found to depend upon the tank geometry and liquid viscosity. Sun *et al.*[8] developed an equivalent TMD model with amplitude-dependent mass, frequency and damping calculated using empirical results for the control force and excitation amplitude directly. That is, the energy dissipation equivalence described in the previous section was not used in their analysis. Figure 6 provides a comparison of mass, damping and frequency ratios for rectangular and circular tanks of the Sun *et al.*[8] study with those of the present investigation. The present results for damping and frequency ratios fall in-between those obtained by Sun *et al.*[8] for water and the higher viscosity liquid results. It can be seen that although the initial effective mass is 80 per cent of the total liquid mass for Sun's model, the effective mass increases to 100 per cent as amplitude of excitation increases. This result does not hold true for the circular tank investigation where the liquid mass participation in the sloshing motion is different. Although the non-linearity of the sloshing motion is evident, the plots of the parameters vs. amplitude of excitation suggests that the values "level" off at some maximum for larger amplitude excitation. It is noted that all of the circular tank results and all but one of the

 

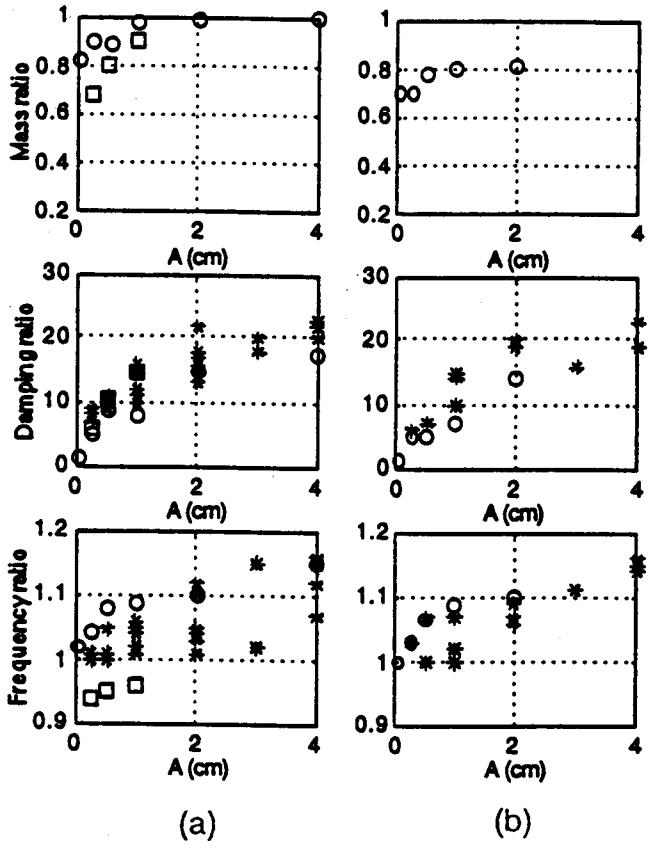


Figure 6. Comparison of the equivalent TMD model of Sun *et al.*[8] (○ for water; □ for liquid with viscosity 11·2 times greater than that of water) with the NSD results (* water): (a) rectangular tanks; (b) circular tanks

rectangular tank results of the Sun *et al.*[8] study fall into the weak wave breaking range of $A/L < 0{\cdot}03$. Because of this limitation, the dramatic change in the stiffness (frequency) parameter for strong wave breaking displayed in Figure 5 is not apparent based on their results even when they are examined in terms of the non-dimensional amplitude. In this regard, the present investigation has shown that the weak wave breaking results may not be simply extended for the strong wave breaking region, but rather, that the laboratory tests for large amplitude excitation were required to identify the nature of the parameter changes that reflect the underlying physical phenomenon. Because large amplitude excitation is assumed to be indicative of earthquake motion, this finding has important implications for design.

Before examining the results of numerical simulations of the control provided by the TLD through the NSD model for a single-degree-of-freedom system, the general algorithm for determining the time-varying non-linear parameters will be derived. The specific results for harmonic and random excitation will then be considered.

 

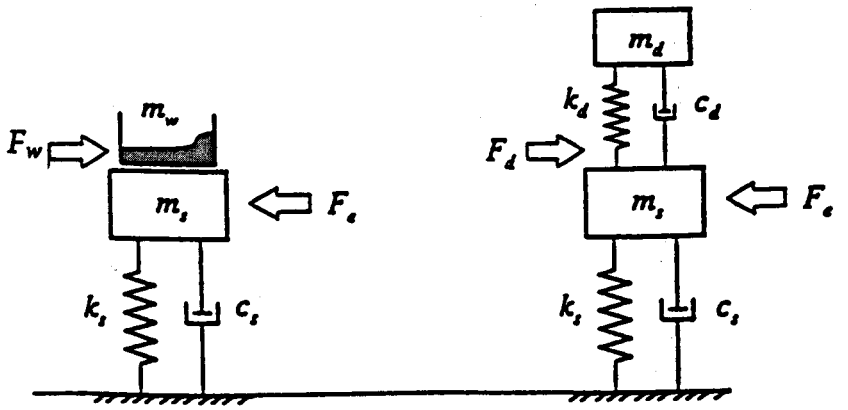


Figure 7. A schematic of the 2-DOF system used in evaluating structural behaviour with the NSD model of the TLD

*Parameter modification under general excitation conditions*

A Two-Degree-of-Freedom system (2DOF) is used to evaluate the motion of a structure with an attached control system. Because the time-varying excitation will influence the tank sloshing motion of the TLD, the corresponding stiffness and damping properties of the NSD must be continuously updated. An algorithm to update the NSD parameters at each time step as a function of the base excitation amplitude is required. In the algorithm for a SDOF structural system, this amplitude is taken to be the structural displacement at the previous time step. In other words, the amplitude $A$ used in the definition of $\Lambda$ in Figures 4 and 5 is the structural displacement $x_s$ in this case. A schematic of the 2-DOF model is shown in Figure 7. The equations of motion in matrix form are

$$\begin{bmatrix} m_d & 0 \\ 0 & m_s \end{bmatrix} \begin{Bmatrix} \ddot{x}_d \\ \ddot{x}_s \end{Bmatrix} + \begin{bmatrix} c_d & -c_d \\ -c_d & c_d + c_s \end{bmatrix} \begin{Bmatrix} \dot{x}_d \\ \dot{x}_s \end{Bmatrix} + \begin{bmatrix} k_d & -k_d \\ -k_d & k_d + k_s \end{bmatrix} \begin{Bmatrix} x_d \\ x_s \end{Bmatrix} = \begin{Bmatrix} 0 \\ F_e \end{Bmatrix} \tag{14}$$

where $m$, $c$, $k$, $x$, $\dot{x}$ and $\ddot{x}$ are the mass, damping, stiffness, relative displacement, velocity and acceleration, respectively. The subscripts d and s indicate the damper and the structure, respectively. The parameters $m_s$, $m_d$, $c_s$, and $k_s$ are assumed to be given in this scheme. The amplitude of the external forcing function $F_e$ is approximated to be a constant at each time step of the numerical procedure. The damping and stiffness coefficients of the control system are determined using equations (10) and (11). Figure 8 summarizes the scheme.

*Results for harmonic excitation*

A SDOF system equipped with a TLD is modeled as a 2-DOF system with the NSD representing the TLD. The properties of the NSD are functions of the peak amplitude of the structural motion as described in equations (10) and (11). As the structure is subjected to harmonic excitation, the peak amplitude becomes a constant at steady state. The properties of the

 

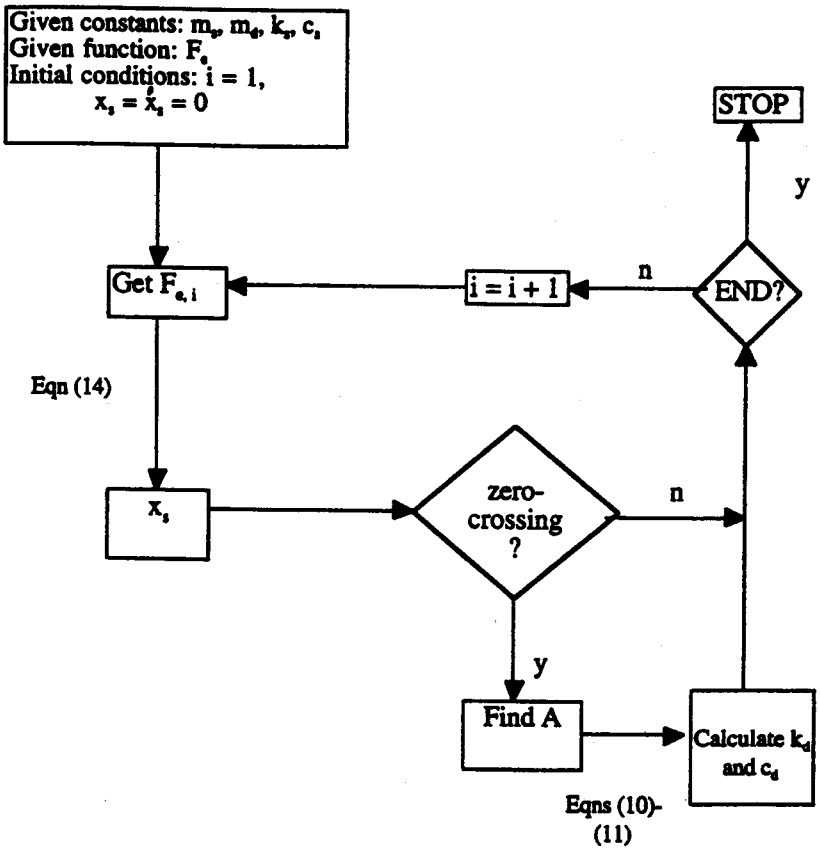


Figure 8. The algorithm for estimating structural behaviour using the NSD model

NSD therefore become constant at steady state. Figures 9(a) and 9(b) show the numerically simulated time histories of the damping and stiffness hardening parameters, respectively, for the NSD model attached to a sinusoidally excited structure with the following structural properties:

$$f_s = 0{\cdot}32 \text{ Hz}, \qquad \zeta_s = 1{\cdot}0 \text{ per cent}, \qquad \mu = 1{\cdot}0 \text{ per cent}$$

where $\mu$ is the ratio of the total effective mass of the damper to the structural mass. A value of 1 per cent is usually assumed as larger values prohibitively increase the dead load demand on the structure. The time histories are generated for a forcing function with frequency near the jump frequency ratio of 1·1. These figures clearly show the parameters approach the constant steady-state values very quickly and remain constant.

*Results for white noise excitation*

In this section, the behaviour of the TLD coupled with a lightly damped SDOF system is investigated numerically for white noise excitation. There were no shaking table data available for

 

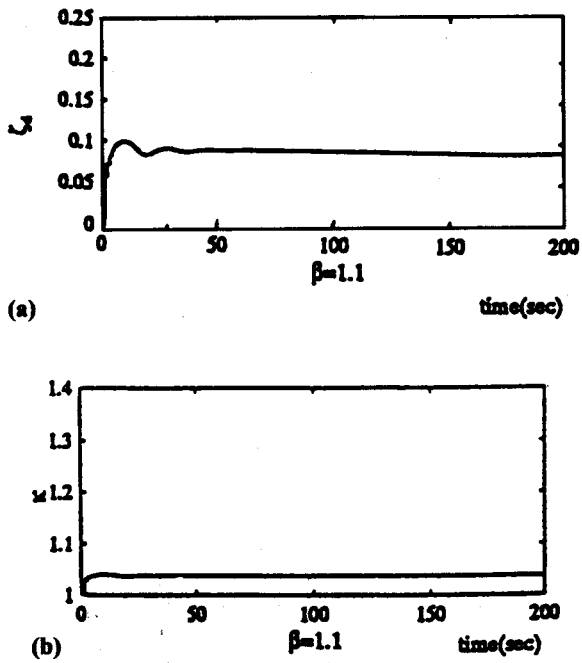


Figure 9. (a) The time varying behaviour of the damping ratio under sinusoidal excitation; (b) the time varying behaviour of the stiffness-hardening ratio under sinusoidal excitation

comparison. As the structure is subjected to a random forcing function with a constant spectral density, i.e. white noise, the equation of motion is solved at each time step. Sample time histories of generated white noise excitation of a lightly damped structure appear in Figures 10(a) and 10(b), for the same structural system evaluated under harmonic excitation cited previously, $f_s = 0{\cdot}32$ Hz, $\zeta_s = 1{\cdot}0$ per cent, $\mu = 1{\cdot}0$ per cent. For these conditions, Figures 10(c) and 10(d) show sample time histories of the damping and stiffness ratios of the NSD, respectively. These parameters are obtained by updating the algorithm in Figure 8 at each time step with the previously determined peak structural displacement. The NSD model provided an average 27 per cent reduction in the peak structural displacement for the 50 sets of simulated white noise excitation undertaken. This analysis showed that the relationships provided in Figures 4 and 5 for modifying parameters are adequate under white noise forcing even though they are based upon the shaking table experiments for harmonic excitation.

*Results for seismic excitation*

In this section, the results of shaking table experiments using the well-known El Centro ground acceleration are discussed. Ground motion records of the 1946 El Centro earthquake were numerically imposed on a SDOF system whose natural frequency is 0·5 Hz. The dynamic response of this structure was obtained such that the maximum displacement was within the range of the shaking table used, approximately 40 mm. The shaking table motions derived from

 

this exercise are shown in Figure 11(a). A TLD with length $L$ of 590 mm, water depth of 36 mm, whose linear natural frequency is 0·506 Hz was mounted on the shaking table and subjected to this record. The base shear or control force generated by the TLD during the entire excitation period was measured and recorded with a solid line in Figure 11(b) and the corresponding energy dissipation per half-cycle was plotted in Figure 11(c). The NSD model employed for the TLD was subjected to the same excitation record as that provided by the shaking table. The dynamic response of the NSD was obtained numerically. The time history of the base shear generated by the NSD is presented in Figure 11(b) by the dashed line. The corresponding energy dissipation per half-cycle is shown by a dotted line in Figure 11(c) also. In both plots, it is apparent that the solid and dashed curves are in close agreement, with the NSD model providing a slightly higher control

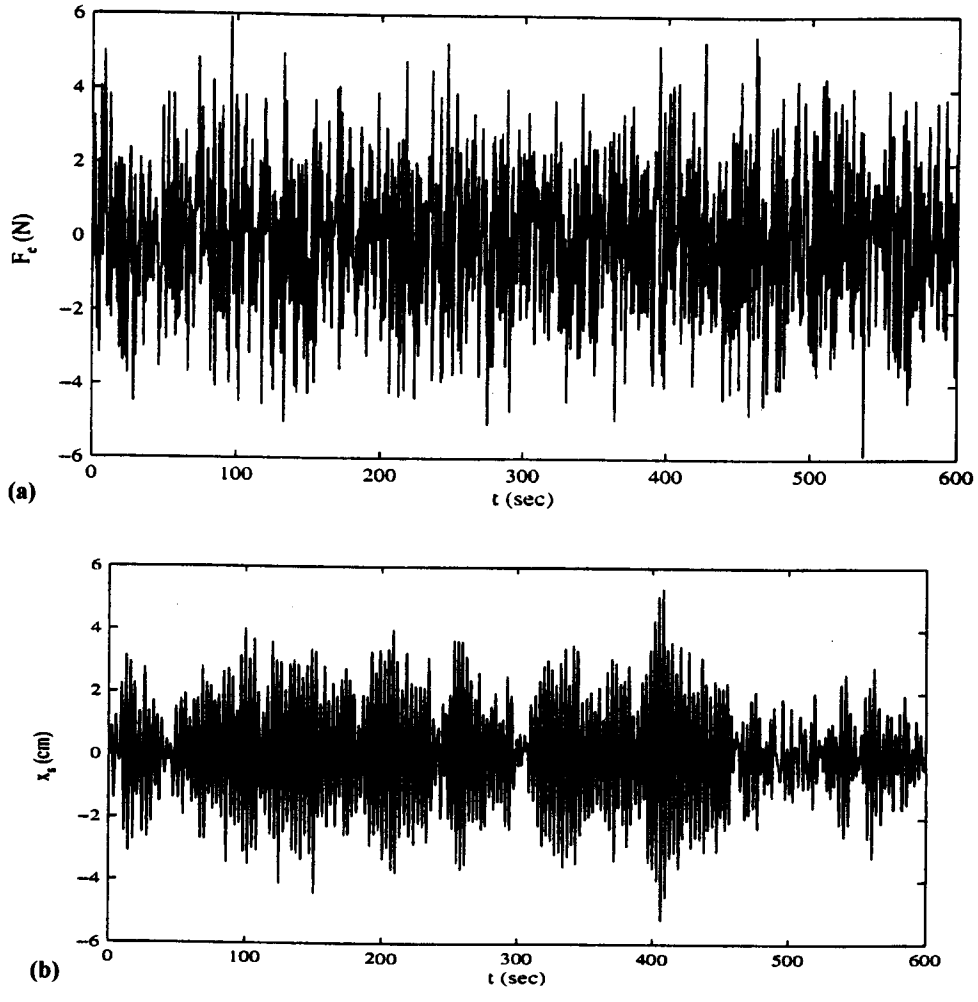


Figure 10. (a) White noise excitation; (b) structural displacement induced by white noise excitation; (c) damping ratio, $\zeta_d$; (d) stiffness hardening ratio, $\kappa$

 

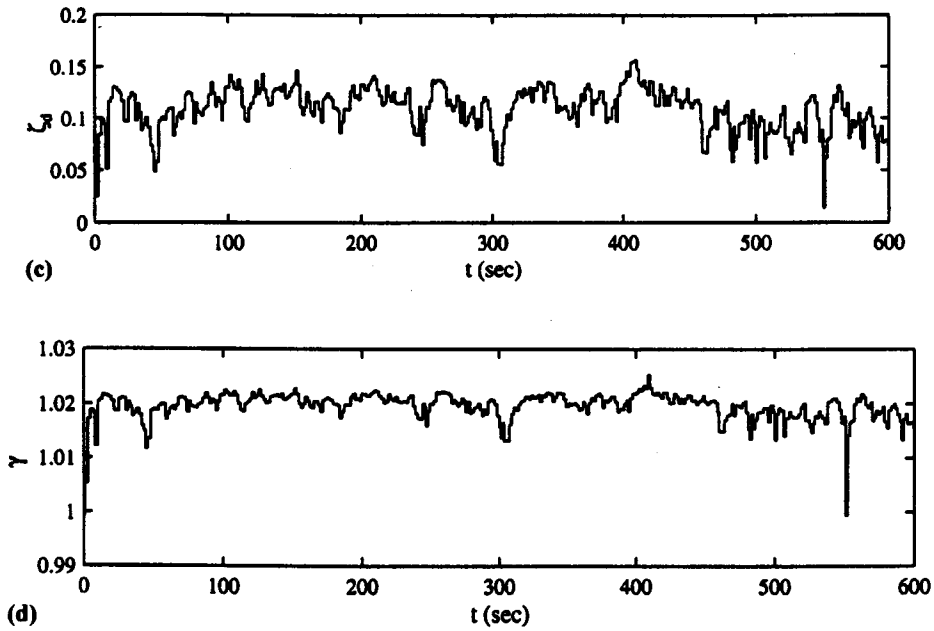


Figure 10. (*Continued*)

force. The damping and stiffness hardening ratios during the excitation period are shown in Figures 11(d) and 11(e), respectively. Although the stiffness hardening parameter appears to have greater variation with respect to time, both parameters eventually level off. These preliminary results suggest that the NSD adequately characterizes the behaviour of the TLD under seismic loading conditions.

## DESIGN IMPLICATIONS

In TLD design, tank size and water depth are selected based upon the estimate of the required control force. The effectiveness of the damping device in reducing the peak displacement of the structure is the primary objective. The NSD model provides an initial estimate of the nonlinearly tuned water depth for maximum effectiveness at a given peak displacement for a given fundamental structural frequency. Further, the relationships derived previously for damping allow the designer to fully characterize the tank parameters for additional numerical analysis. Simulation using the algorithm provided in Figure 8 and presented for various forcing functions discussed in the results section may be applied for additional investigation.

Proper tuning of the tank is essential to achieve maximum effectiveness. The linearly tuned water depth is calculated from equation (6) as

$$h_0 = \frac{L}{\pi} \tanh^{-1}\left(\frac{4\pi L f_s^2}{g}\right) \tag{15}$$

 

The non-linear tuning frequency is expressed as

$$f_d = \frac{\xi}{2\pi}\sqrt{\frac{\pi}{L}\tanh\left(\frac{\pi h_0}{L}\right)} \tag{16}$$

which includes the stiffness hardening parameter. Solving equation (16) for the water depth yields

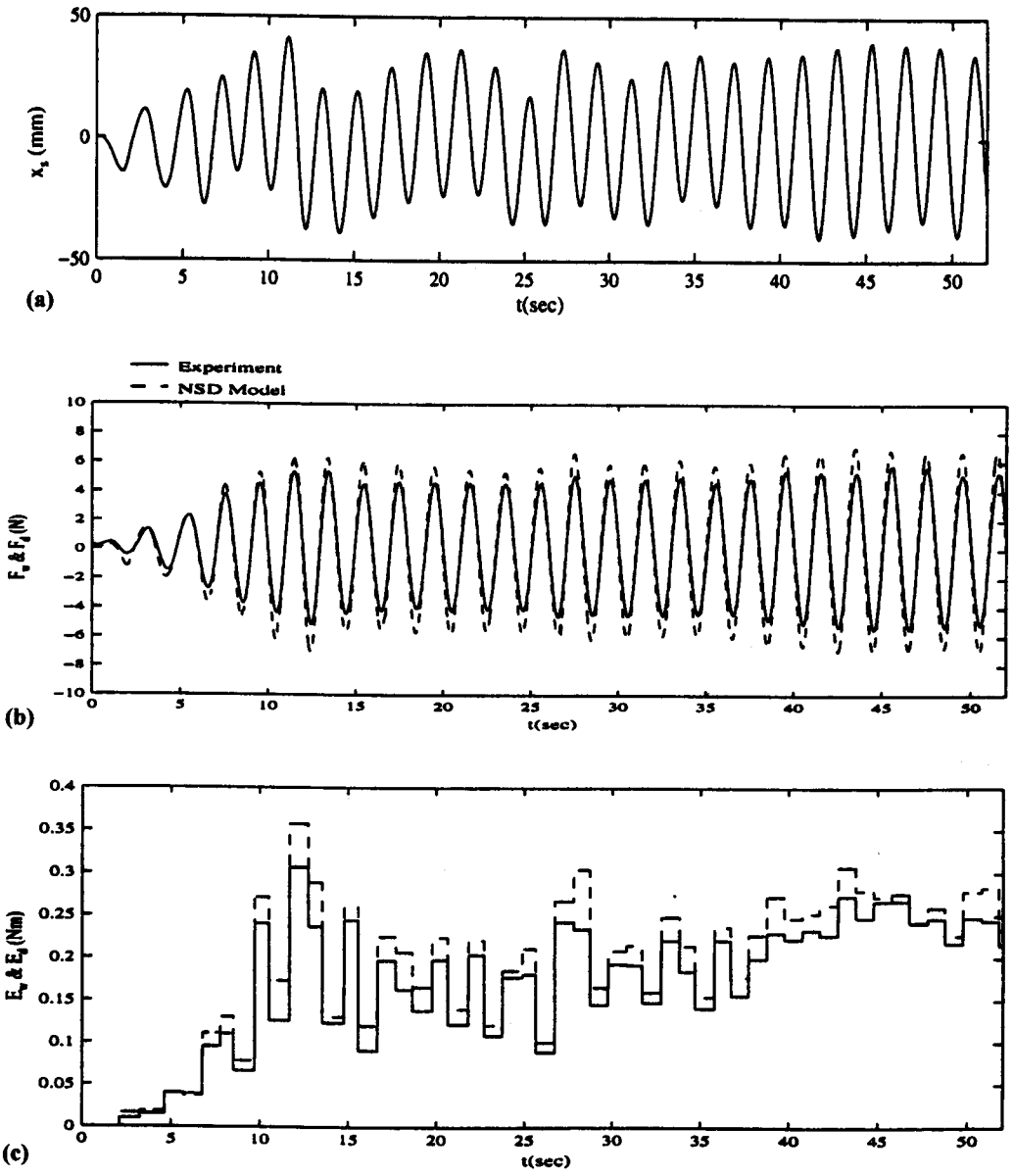


Figure 11. (a) Scaled structural displacement; (b) damping forces; (c) energy dissipation per cycle; (d) damping ratio, $\zeta_d$; (e) stiffness hardening ratio, $\kappa$

 

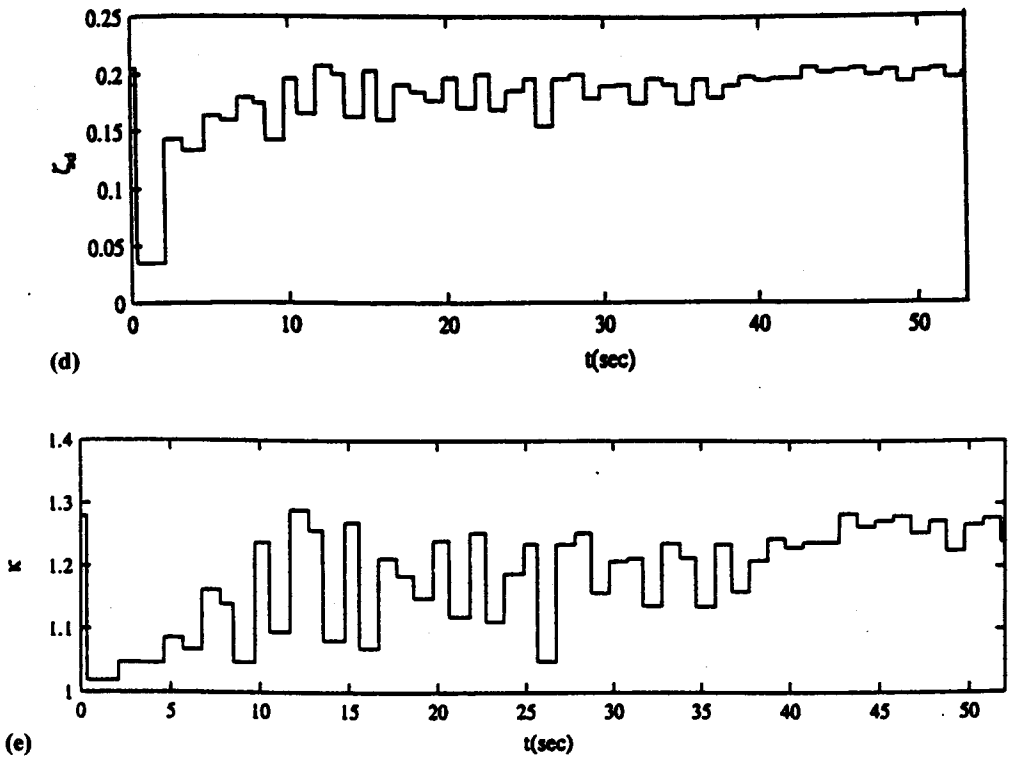


Figure 11. (*Continued*)

the following expression:

$$h_0 = \frac{L}{\pi} \tanh^{-1}\left(\frac{4\pi L f_s^2}{g\xi^2}\right) \tag{17}$$

If the peak structural amplitude can be estimated beforehand, the water depth can be calculated; otherwise an iterative procedure is required. Because the damping parameter is also a function of the peak excitation amplitude and tank length, it can also be estimated for a given system through equation (10).

## CONCLUSIONS

The NSD model presented here is an equivalent TMD representation of the TLD. The model is obtained from a scheme based upon energy dissipation equivalence. The NSD model relies in part upon an empirically derived stiffness-hardening parameter. Because the stiffness and damping parameters of the model are derived from tests of tanks subjected to large amplitudes of excitation, they are considered to be more representative of behaviour for earthquake excitation

 

than those previously obtained for smaller amplitudes of excitation. In addition, because structural engineers are concerned with control under extreme loadings, these large amplitude results are important for the development of design guidelines. An algorithm for updating the NSD coefficients in a time history analysis of a SDOF structural system has been provided. The procedure clearly has merit as a design tool for liquid dampers.

## ACKNOWLEDGEMENTS

This work described here partially fulfilled the requirements of the doctor of philosophy degree in Civil Engineering for the first author. Suggestions made by Prof. Harry Yeh of the University of Washington and Prof. Y. Tamura of the Tokyo Institute of Polytechnics were very useful. The support of the U.S. National Science Foundation for this project is gratefully acknowledged.

## REFERENCES

1. D. A. Reed, H. Yeh, J. Yu and S. Gardarsson, 'Experimental investigation of tuned liquid dampers', *Proc. ASCE 1996 Int. Conf. on Natural Disaster Reduction*, Washington, DC, December (1996a).
2. D. A. Reed, H. Yeh, J. Yu and S. Gardarsson, 'Performance of tuned liquid dampers for large amplitude excitation', *Proc. 2nd Int. Workshop on Structural Control*, Hong Kong, December (1996b).
3. A. A. Fediw, B. Breukelman, D. P. Morris and N. Isyumov, 'Effectiveness of a tuned sloshing water damper to reduce the wind-induced response of tall building', *Proc. 7th U.S. National Conf. of Wind Engineering*, Vol. 1, Los Angeles, CA, 27–20 June 1993, pp. 233–242.
4. K. Fujii, Y. Tamura, T. Sato and T. Wakahara, 'Wind-induced vibration of tower and practical applications of tuned sloshing damper', *J. Wind Engng. Ind. Aerodyn.* **33**, 263–272 (1990).
5. Y. Tamura, K. Fuji, T. Sato, T. Wakahara and M. Kosugi, 'Wind-induced vibration of tall towers and practical applications of tuned sloshing dampers', *Proc. Symp. on Serviceability of Buildings*, Vol. 1, Univ. of Ottawa, Ottawa, Canada, May p 188.
6. T. Wakahara, T. Ohyama and K. Fujii, 'Suppression of wind-induced vibration of a tall building using the tuned-liquid dampers', *J. Wind Engng. Ind. Aerodyn.* **41-44**, 1895–1906 (1992).
7. T. Wakahara, 'Wind-induced response of TLD-structure coupled system considering nonlinearity of liquid motion', *Shimizu Tech. Res. Bull.* (12), 41–52 (1993).
8. L. M. Sun, Y. Fujino, P. Chaiseri and B. M. Pacheco, 'The properties of tuned liquid dampers using TMD analogy', *Earthquake Engng. Struct. Dyn.* **24**, 967–976 (1995).
9. J.-K. Yu, 'Nonlinear characteristics of tuned liquid dampers', *Ph.D. Thesis*, University of Washington, Department of Civil Engineering, Seattle, WA, 98195, 1997.
10. H. Lamb, *Hydrodynamics*, The University Press, Cambridge, England (1932).
11. L. Sun, 'Semi-analytical modeling of tuned liquid damper (TLD) with emphasis on damping of liquid sloshing', *Ph.D. Thesis*, University of Tokyo, Tokyo, Japan, 1991.
12. Y. Fujino, L. Sun, B M. Pacheco and P. Chaiseri, 'Tuned liquid damper for suppressing horizontal motion of structures', *J. Engng. Mech.* **118**(10), 2017–2030 (1992).
13. D. A. Reed, J. Yu, H. Yeh and S. Gardarsson, 'Experiment and theoretical investigations of tuned liquid dampers', *J. Engng. Mech.* **124**(4), 405–413 (1998).
14. Y. Fujino, B. M. Pacheco, P. Chaiseri, L. M. Sun and K. Koga, 'Understanding of TLD properties based on TMD analogy', *J. Struct. Engng.* JSCE **36**, (1990) (in Japanese).
15. D. A. Reed, 'Structural control using tuned liquid dampers', *Proc. UJNR Workshop on Wind Effects*, University of Hawaii at Manoa, Honolulu, Hawaii, 7–9 October 1997.
16. L. M. Sun, Y. Fujino, B. M. Pacheco, and P. Chaiseri, 'Modeling tuned liquid dampers', *Proc. 8th Int. Conf. on Wind Engineering*, (1991).

 